BATTERIES

Rational design of layered oxide materials for sodium-ion batteries

Chenglong Zhao[1,2]*, Qidi Wang[3,4]*, Zhenpeng Yao[5]*, Jianlin Wang[6], Benjamín Sánchez-Lengeling[5], Feixiang Ding[1,2], Xingguo Qi[1,2], Yaxiang Lu[1,2]†, Xuedong Bai[6], Baohua Li[3], Hong Li[1,2], Alán Aspuru-Guzik[5,7]†, Xuejie Huang[1,2], Claude Delmas[8]†, Marnix Wagemaker[9]†, Liquan Chen[1], Yong-Sheng Hu[1,2,10]†

Sodium-ion batteries have captured widespread attention for grid-scale energy storage owing to the natural abundance of sodium. The performance of such batteries is limited by available electrode materials, especially for sodium-ion layered oxides, motivating the exploration of high compositional diversity. How the composition determines the structural chemistry is decisive for the electrochemical performance but very challenging to predict, especially for complex compositions. We introduce the "cationic potential" that captures the key interactions of layered materials and makes it possible to predict the stacking structures. This is demonstrated through the rational design and preparation of layered electrode materials with improved performance. As the stacking structure determines the functional properties, this methodology offers a solution toward the design of alkali metal layered oxides.

Integration of intermittent renewable energy sources demands the development of sustainable electrical energy storage systems (*1*). Compared with lithium (Li)–ion batteries, the abundance and low cost of sodium (Na) make Na-ion batteries promising for smart grids and large-scale energy storage applications (*2*, *3*). Li-ion layered oxides, with the general formula $LiTMO_2$, have represented the dominant family of electrode materials for Li-ion batteries since 1980 (*4*). TM stands for one or multiple transition metal elements that facilitate the redox reaction associated with Li-ion (de-)intercalation. The layered structures are built up by edge-sharing TMO_6 octahedra, forming repeating layers between which Li ions are positioned in the octahedral (O) oxygen environment, leading to the so-called O-type stacking. The structure offers high compositional diversity, providing tunable electrochemical performance, of which well-known examples are $LiCoO_2$ and Ni-rich $LiNi_yCo_zMn(Al)_{1-y-z}O_2$. In search of electrodes for Na-ion batteries, layered oxides (Na_xTMO_2) offered the natural starting point (*5*). However, a key difference is that for Na-ion oxides, in addition to O-type, P-type stacking can occur, in which P-type refers to prismatic Na-ion coordination (Fig. 1A). These stackings show distinctly different electrode performance, in which the most studied layered stacking configurations are P2 and O3 types (Fig. 1A), referring to the ABBA and ABCABC oxygen stacking, respectively (*6*). P2-type oxides usually provide higher Na-ion conductivity and better structural integrity against the O3 analogs, which is responsible for the high power density and good cycling stability (*7*). However, the lower initial Na content of P2-type electrodes limits the storage capacity in the first charge compared with high-Na-content O3-type materials (*8*). Usually, the structural transition between the O- and P-type can occur upon Na-ion (de)intercalation during (dis)charging, typically degrading cycle stability (*2*, *3*).

In a search for electrodes with good chemical and dynamic stability and high Na storage

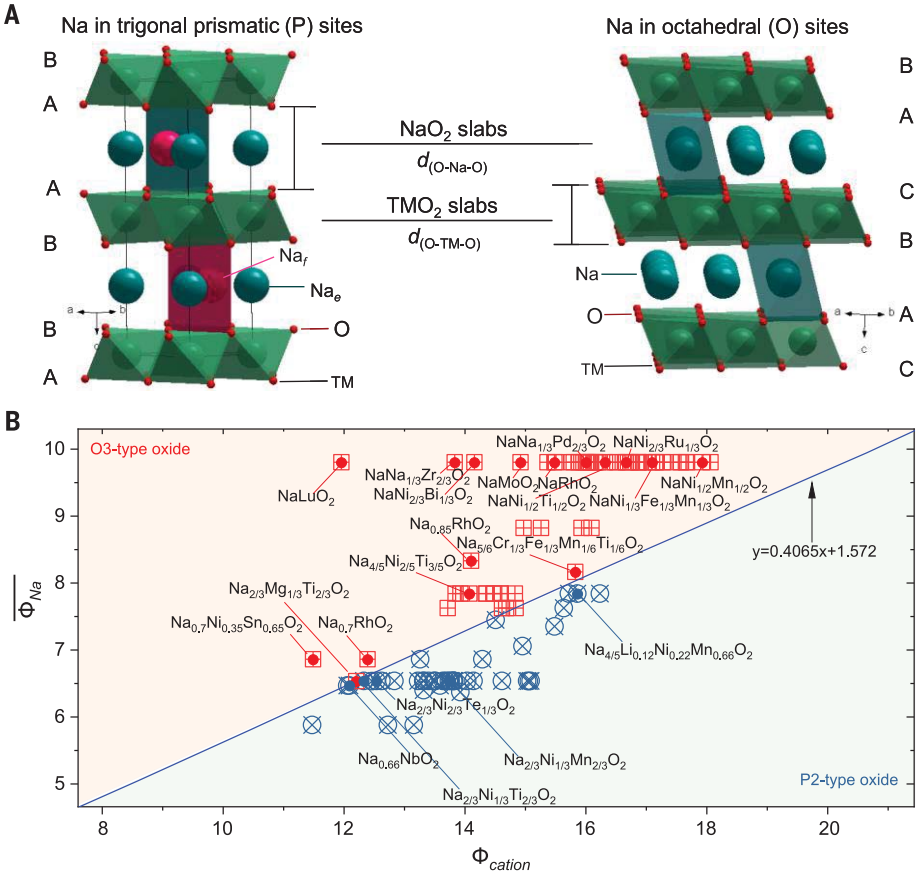

Fig. 1. Cationic potential and its use in Na-ion layered oxides. (**A**) Schematic illustration of crystal representative P2-type (hexagonal) and O3-type (rhombohedral) layered oxides. (**B**) Cationic potential of representative P2- and O3-type Na-ion layered oxides, considering the Na content, oxidation state of transition metals, and TM composition (see supplementary text and fig. S3 for details).

performance, various P2- and O3-type Na-ion layered oxides have been synthesized and investigated (*9*, *10*). However, effective guidelines toward the design and preparation of optimal electrode materials are lacking. Crystal structures of P2- and O3-type layered oxides can be differentiated on the basis of the ratio between the interlayer distance of the Na metal layer $d_{(O\text{-}Na\text{-}O)}$ and the TM layer distance $d_{(O\text{-}TM\text{-}O)}$ (*11*), in which a ratio of ~1.62 distinguishes P2- and O3-type oxides (fig. S1 and table S1) (*12*). The larger ratio of P2-type oxides originates from the more localized electron distribution within the TMO_2 slabs, which results in a weaker repulsion between the adjacent NaO_2 slabs and consequentially a stronger repulsion between the adjacent TMO_2 slabs. This hints that the electron distribution plays an important role in the competition between the P- and O-type stackings in layered oxides.

Ionic potential (Φ) is an indicator of the charge density at the surface of an ion, which is the ratio of the charge number (n) with the ion radius (R) introduced by G. H. Cartledge (*13*), reflecting the cation polarization power. The ionic potential shows the expected increase with oxidation state and atom mass (fig. S2 and table S2), a consequence of the less localized orbitals.

Aiming at a simple descriptor for layered oxides, we express the extent of the cation electron density and its polarizability, normalized to the ionic potential anion (O), by defining the "cationic potential":

$$\Phi_{\text{cation}} = \frac{\overline{\Phi_{\text{TM}}}\,\overline{\Phi_{\text{Na}}}}{\overline{\Phi_{\text{O}}}} \qquad (1)$$

where $\overline{\Phi_{\text{TM}}}$ represents the weighted average ionic potential of TMs, defined as $\overline{\Phi_{\text{TM}}} = \sum \frac{w_i n_i}{R_i}$; w_i is the content of TM_i having charge number n_i and radius R_i; and $\overline{\Phi_{\text{Na}}}$ represents the weighted average ionic potential of Na defined as $\overline{\Phi_{\text{Na}}} = \frac{x}{R_{\text{Na}}}$. Charge balance in Na_xTMO_2 composition demands $\sum w_i n_i = 4 - x$, where x represents Na content and 4 is the total oxidation state to charge compensate O^{2-}.

The cationic potential Φ_{cation} versus the weighted average Na ionic potential $\overline{\Phi_{\text{Na}}}$ of reported P2- and O3-type layered oxides results in the phase map shown in Fig. 1B. The distinct P2- and O3-type regions indicate that the cationic potential is an accurate descriptor of the interslab interaction and, thereby, the structural competition between P2- and O3-type structures. A larger cationic potential (Eq. 1) implies stronger TM electron cloud extend and interlayer electrostatic repulsion resulting in the P2-type structure, with more covalent TM-O bonds and an increased $d_{(O\text{-}Na\text{-}O)}$ distance (fig. S4). Opposing this, a larger mean Na ionic potential, achieved by increasing Na content, increases the shielding of the electrostatic repulsion between the TMO_2 slabs, favoring the O3-type structure.

The phase map (Fig. 1B) shows that very small differences in TM or Na content can

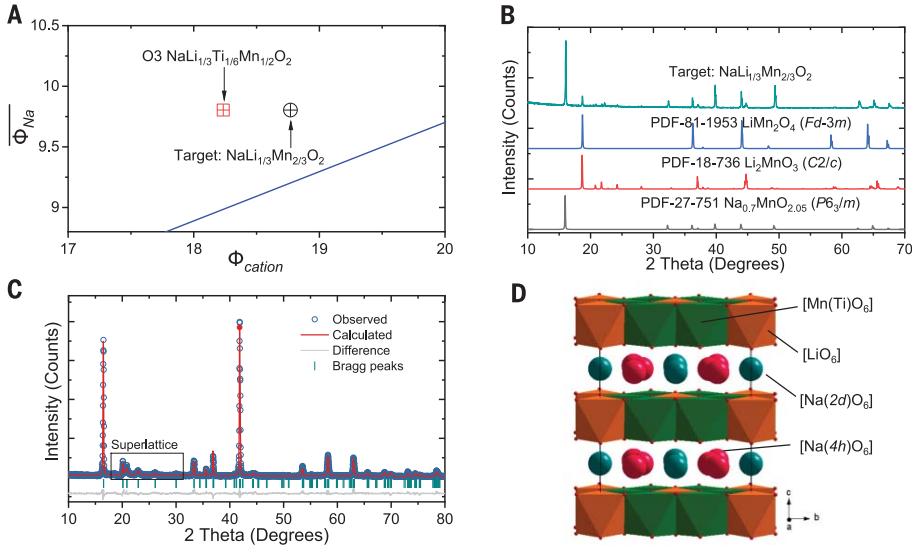

Fig. 2. Designing an O3-type oxide. (**A**) Analysis of the cationic potential of Na-Li-Mn(Ti)-O oxides (see tables S8 and S9 for details). (**B**) XRD patterns of the targeted $NaLi_{1/3}Mn_{2/3}O_2$ and the standard references. (**C**) Rietveld refinement of XRD pattern of $NaLi_{1/3}Ti_{1/6}Mn_{1/2}O_2$ (see tables S10 to S12 for details). (**D**) Schematic illustration of the corresponding structure with the Li/Mn(Ti) ordering in the $[Li_{1/3}Ti_{1/6}Mn_{1/2}]O_2$ slabs.

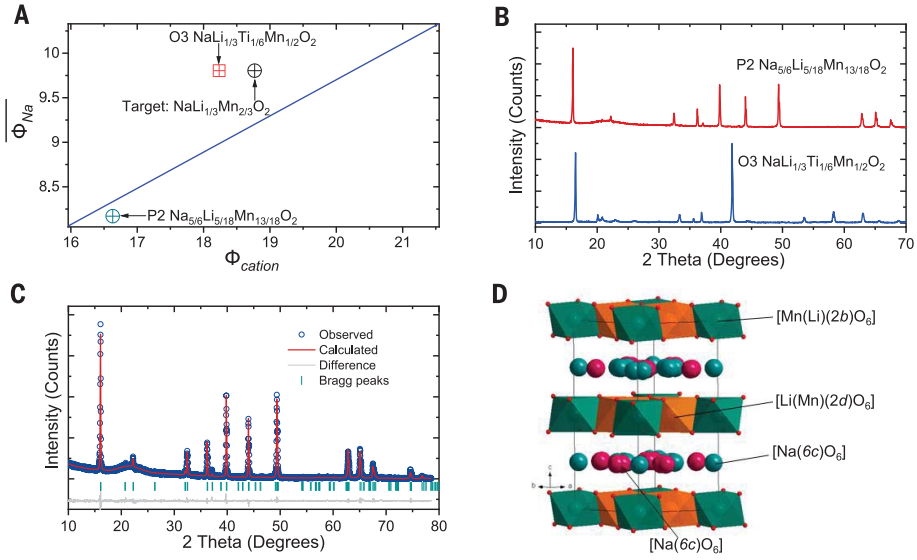

Fig. 3. Designing a P2-type oxide. (**A**) Analysis of cationic potential of Na-Li-Mn-O oxides (see tables S13 and S14 for details). (**B**) XRD patterns of $NaLi_{1/3}Ti_{1/6}Mn_{1/2}O_2$ and $Na_{5/6}Li_{5/18}Mn_{13/18}O_2$ oxides. (**C**) Rietveld refinement of XRD pattern of $Na_{5/6}Li_{5/18}Mn_{13/18}O_2$ (see tables S15 to S17 for details). (**D**) Schematic illustration of the corresponding structure with the Li/Mn ordering in the $[Li_{5/18}Mn_{13/18}]O_2$ slabs.

[1]Key Laboratory for Renewable Energy, Beijing Key Laboratory for New Energy Materials and Devices, Beijing National Laboratory for Condensed Matter Physics, Institute of Physics, Chinese Academy of Sciences, Beijing 100190, China. [2]Center of Materials Science and Optoelectronics Engineering, University of Chinese Academy of Sciences, Beijing 100049, China. [3]Shenzhen Key Laboratory on Power Battery Safety and Shenzhen Geim Graphene Center, School of Shenzhen International Graduate, Tsinghua University, Guangdong 518055, China. [4]School of Materials Science and Engineering, Tsinghua University, Beijing 100084, China. [5]Department of Chemistry and Chemical Biology, Harvard University, Cambridge, MA 02138, USA. [6]State Key Laboratory for Surface Physics, Institute of Physics, Chinese Academy of Sciences, Beijing, 100190, China. [7]Department of Chemistry and Department of Computer Science, University of Toronto, Toronto, Ontario M5S 3H6, Canada. [8]Université de Bordeaux, Bordeaux INP, ICMCB UMR 5026, CNRS, 33600 Pessac, France. [9]Department of Radiation Science and Technology, Delft University of Technology, Mekelweg 15, 2629JB Delft, Netherlands. [10]Yangtze River Delta Physics Research Center, Liyang 213300, China.
*These authors contributed equally to this work.
†Corresponding author. Email: yxlu@iphy.ac.cn (Y.L.); aspuru@utoronto.ca (A.A.-G.); delmas@icmcb-bordeaux.cnrs.fr (C.D.); m.wagemaker@tudelft.nl (M.W.); yshu@iphy.ac.cn (Y.S.-H.)

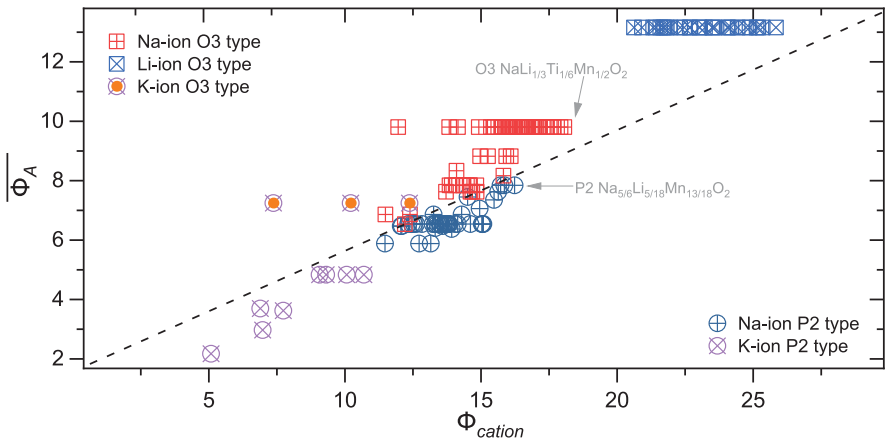

Fig. 4. Cationic potential phase map for alkali metal layered oxides. Summary of reported alkali metal layered materials including Li-/Na-/K-ion oxides (see tables S18 and S19 for details).

result in a transition between P2- and O3-type structures. To illustrate this, we consider layered oxides with the composition $Na_{2/3}TMO_2$, which typically crystallizes in a P2-type structure for the low Na content, such as P2-$Na_{2/3}CoO_2$ (*14*) or P2-$Na_{2/3}Ni_{1/3}Ti_{2/3}O_2$ (*15*). However, replacing Ni^{2+} with Mg^{2+} in P2-$Na_{2/3}Ni_{1/3}Ti_{2/3}O_2$, facilitated by their similar ionic radii (*16*), leads to $Na_{2/3}Mg_{1/3}Ti_{2/3}O_2$, for which the cationic potential predicts the O3-type structure, which is difficult to predict even with complex electrostatic energy calculations (*15*). In this case, the smaller ionic potential of Mg^{2+} against Ni^{2+} (Fig. 1B) decreases Φ_{cation}; the resulting lower covalence of Mg/Ti-O bonds increases the charge carried by the oxygens and thereby weakens the repulsion between the TM layers, resulting in an O3-type structure (fig. S5, A and B, and tables S6 and S7). Substituting 1/6 Mg^{2+} by Ni^{2+} in $Na_{2/3}Mg_{1/3}Ti_{2/3}O_2$ to $Na_{2/3}Ni_{1/6}Mg_{1/6}Ti_{2/3}O_2$ moves it back into a P2-type structure (fig. S5B), illustrating how near these compositions are to the line separating the P2- and O3-type phases. Several other examples demonstrating that the proposed cationic potential approach captures the subtle balance between the P2- and O3-type layered Na_xTMO_2 structures are provided in the supplementary text and figs. S5C and S6.

Delmas *et al.* (*6*, *17*) used the Rouxel diagram (*18*) to distinguish Na_xTMO_2 stacking structures, demonstrating that both Na content and the ionicity and covalence of bonds are the important factors. However, this method only accounts for the difference in Pauling's electronegativity (fig. S7 and table S4), which makes it impossible to predict the structure of oxides with the same TMs in different oxidation states (*6*, *17*) (e.g., Mn^{4+} and Mn^{3+} in $Na_{0.7}MnO_2$) or for multiple-component systems (see supplementary text, fig. S8, and table S5 for details). The cationic potential correctly predicts the stacking structure for these cases, providing a guideline for the development of Na-ion layered oxides.

Using the cationic potential as a guide, we design specific stacking structures by controlling the Na content and TM composition. A notable starting point is $NaLi_{1/3}Mn_{2/3}O_2$, the analog of $LiLi_{1/3}Mn_{2/3}O_2(Li_2MnO_3)$, providing capacity on the basis of oxygen redox chemistry. This composition has not been prepared so far, although theoretical calculations argue $NaLi_{1/3}Mn_{2/3}O_2$ is stable in an O3-type structure (*19*). Various experimental conditions were attempted to prepare this composition in an O3-type structure, but always a P2-type component, in addition to other phases, was obtained. Lowering the cationic potential suggests that a possible route to prepare the O3-type structure is partial substitution of Mn^{4+} by Ti^{4+} (Fig. 2A), where Ti^{4+} has a lower ionic potential. $NaLi_{1/3}Ti_{1/6}Mn_{1/2}O_2$ was successfully prepared in the predicted O3-type structure by a typical solid-state reaction (materials and methods). Notably, $NaLi_{1/3}Mn_{2/3}O_2$ could not be synthesized as an O3-type structure by using the same method (Fig. 2B). Rietveld refinement of the x-ray diffraction (XRD) pattern confirmed the layered rock-salt structure (Fig. 2C), in which the NaO_2 layers alternate with the mixed $[Li_{1/3}Ti_{1/6}Mn_{1/2}]O_2$ slabs (Fig. 2D). The (*1/3*, *1/3*, *l*) superstructure peaks in 20° to 30° suggest Li/Mn(Ti) ordering in a honeycomb pattern, which is also confirmed by the aberration-corrected scanning transmission electron microscopy (fig. S9). This ordered arrangement of Li and Mn(Ti) in the TMO_2 slabs has not been observed in O3-type Na-ion oxides with exclusively 3d TMs. The electrochemical properties (see supplementary text and fig. S10A for details) demonstrate an energy density of ~630 watt-hours (Wh) kg^{-1}, higher than that of the reported O3-type electrodes.

We then use cationic potential to design a P2-type structure aiming at an anomalous high Na-content of $x > 0.67$, again starting from $NaLi_{1/3}Mn_{2/3}O_2$. To avoid formation of an O3-type structure, the dividing line in Fig. 1B demonstrates that we should increase the cationic potential (Eq. 1), assuming that Na content remains constant, which can be realized by increasing the ionic potential at TM sites. On the basis of the cationic potential, a P2-type structure with $x = 1$ ($\overline{\Phi_{Na}} = 9.8$) will demand an extremely large TM ionic potential (larger than that of Mn^{4+}, having the largest value among the widely used TMs). Therefore, the Na content in $NaLi_{1/3}Mn_{2/3}O_2$ should be lowered, which can be achieved through charge compensation by decreasing the Li and increasing the Mn content. Following this route, the cationic potential predicts that $Na_{5/6}Li_{5/18}Mn_{13/18}O_2$ composition with high Na content should have the P2-type structure (Fig. 3A), which was indeed successfully prepared (Fig. 3B). So far, layered oxides prepared with such high Na content usually crystallize as an O3-type structure. Compared with the O3-type $NaLi_{1/3}Ti_{1/6}Mn_{1/2}O_2$, the (002) peak of the P2-type structure shifts toward lower diffraction angles, indicating the expected increase in the *c* axis of the unit cell (Fig. 3B). Rietveld refinement of the XRD pattern reveals that this P2-type layered structure can be indexed in the hexagonal $P6_3$ space group (Fig. 3, C and D). The electron energy loss spectroscopy mapping reveals a uniform distribution of the Na, Mn, and O elements in the platelike particles (fig. S11). This as-prepared high-Na-content material has a considerably higher capacity of >200 milliampere-hours (mAh) g^{-1} (fig. S10B).

Extending the cationic potential to other alkali metal layered oxides, Li ion (fig. S12) and K ion (fig. S13), results in phase maps shown in Fig. 4. The cationic potential (Eq. 1) is found to increase from K to Na to Li ion owing to the increasing ability to shield the TMO_2 interslab interaction. As a consequence, K_xTMO_2 mainly crystallizes as the P2-type and Li_xTMO_2 as the O3-type structure, whereas Na_xTMO_2 is the most notable family, as the shielding strength is at the tipping point between P2- and O3-type structures. The distribution of reported layered electrodes exhibits a clear trend by clustering around the dividing line (Fig. 4). For more than 100,000 new compositions, up to quaternary compositions on the TM position, the cationic potential is used to calculate the most stable stacking structure, resulting in a distribution of compositions in the phase map around the dividing line (see figs. S14 and S15 and supplementary text for details). This demonstrates how the cationic potential can be used to predict the structure of new Na_xTMO_2 layered materials, on the basis of specific compositional demands. It is worth noting that the other parts far away from the line may also lead to other types of TM-oxide phases (e.g., rock salt, spinel), or may not lead to stable structures at all, which is the subject of ongoing investigations.

In summary, the ionic potential is a measure of the polarization of ions, mainly reflecting the influence of electrostatic energy on the system. Because the main difference between P- and O-type structures is the electrostatic polarization between AO_2 (A, alkali metals) and TMO_2 slabs, we can apply the proposed cationic potential method to distinguish and design materials, especially useful for Na-ion layered oxides. For entropy-dominated phases, disordered compounds resulting from mechanical milling (*20*), or oxides prepared under particular conditions (*21*, *22*), metastable structures, or nonequilibrium phases (*23*), as well as the local distortion of TMs (e.g., due to Jahn-Teller effect on Mn^{3+}), the cationic potential approach does not provide a sensible guideline. Moreover, the cationic potential only predicts whether the proposed material will crystallize in a P- or O-type structure, and one composition has only one structure. The actual obtained phases depend strongly on the nature of precursors and the conditions/atmosphere of thermal treatment, among others, which may cause the difference in stoichiometry and dynamic process, leading to structural changes. Further structural information is required to decide whether the corresponding material is stable and/or synthesizable in practice and calls for extensive investigation. Additionally, prediction of stacking structures is challenging for density functional theory methods because of the difficulty of predicting the localized nature of TM orbitals, especially for complicated TM compositions that have an enormous configurational space. We demonstrated the use of cationic potentials to tune the TMO_2 interslab interaction, contributing to the important categories of layered materials. The currently known layered materials are either low-Na-content (x = 2/3) P2-type oxides or high-Na-content (x = 1) O3-type oxides; we suggest further exploration of high-Na-content P2-type oxides and low-Na-content O3-type oxides through the as-proposed cationic potential.

REFERENCES AND NOTES

1. B. Dunn, H. Kamath, J.-M. Tarascon, *Science* **334**, 928–935 (2011).
2. S.-W. Kim, D.-H. Seo, X. Ma, G. Ceder, K. Kang, *Adv. Energy Mater.* **2**, 710–721 (2012).
3. M. H. Han, E. Gonzalo, G. Singh, T. Rojo, *Energy Environ. Sci.* **8**, 81–102 (2015).
4. K. Mizushima, P. C. Jones, P. J. Wiseman, J. B. Goodenough, *Mater. Res. Bull.* **15**, 783–789 (1980).
5. N. Yabuuchi *et al.*, *Nat. Mater.* **11**, 512–517 (2012).
6. C. Delmas, C. Fouassier, P. Hagenmuller, *Physica B+C* **99**, 81–85 (1980).
7. C. Fouassier, C. Delmas, P. Hagenmuller, *Mater. Res. Bull.* **10**, 443–449 (1975).
8. S. Komaba *et al.*, *Inorg. Chem.* **51**, 6211–6220 (2012).
9. J. M. Paulsen, R. A. Donaberger, J. R. Dahn, *Chem. Mater.* **12**, 2257–2267 (2000).
10. J. Billaud *et al.*, *Energy Environ. Sci.* **7**, 1387–1391 (2014).
11. M. Guilmard, L. Croguennec, C. Delmas, *J. Power Sources* **150**, A1287–A1293 (2003).
12. C. Zhao, M. Avdeev, L. Chen, Y.-S. Hu, *Angew. Chem. Int. Ed.* **57**, 7056–7060 (2018).
13. G. H. Cartledge, *J. Am. Chem. Soc.* **50**, 2855–2863 (1928).
14. C. Delmas, J.-J. Braconnier, C. Fouassier, P. Hagenmuller, *Solid State Ion.* **3-4**, 165–169 (1981).
15. Y.-J. Shin, M.-Y. Yi, *Solid State Ion.* **132**, 131–141 (2000).
16. G. Singh *et al.*, *Chem. Mater.* **28**, 5087–5094 (2016).
17. C. Delmas, C. Fouassier, P. Hagenmuller, *Mater. Res. Bull.* **11**, 1483–1488 (1976).
18. J. Rouxel, *J. Solid State Chem.* **17**, 223–229 (1976).
19. D. Kim, M. Cho, K. Cho, *Adv. Mater.* **29**, 1701788 (2017).
20. T. Sato, K. Sato, W. Zhao, Y. Kajiya, N. Yabuuchi, *J. Mater. Chem. A Mater. Energy Sustain.* **6**, 13943–13951 (2018).
21. T. Uyama, K. Mukai, I. Yamada, *Inorg. Chem.* **58**, 6684–6695 (2019).
22. M. H. Han *et al.*, *Electrochim. Acta* **182**, 1029–1036 (2015).
23. M. Bianchini *et al.*, *Nat. Mater.* **19**, 1088–1095 (2020).

ACKNOWLEDGMENTS

Funding: This work was supported by the National Natural Science Foundation of China (51725206, 51421002, 21773303), National Key Technologies R&D Program of China (2016YFB0901500), the Strategic Priority Research Program of the Chinese Academy of Sciences (XDA21070500), Youth Innovation Promotion Association, Chinese Academy of Sciences (2020006), Beijing Municipal Science and Technology Commission (Z181100004718008), Beijing Natural Science Fund-Haidian Original Innovation Joint Fund (L182056), and the Netherlands Organization for Scientific Research (NWO) (under the VICI grant no. 16122). Computations were performed on the Niagara supercomputer at the SciNet HPC Consortium. SciNet is funded by the Canada Foundation for Innovation; the Government of Ontario, Ontario Research Fund-Research Excellence, and the University of Toronto. C.Z. also thanks to the State Scholarship Fund of China Scholarship Council (CSC). **Author contributions:** Y.-S.H. conceived this research and supervised this work with M.W., C.Z., and Q.W., who conceptualized the ionic potential method and developed the calculation on examples of Na-/Li-/K-ion layered oxides. C.Z. and Q.W. performed synthesis procedures, experimental investigation of $NaLi_{1/3}Ti_{1/6}Mn_{1/2}O_2$ and $Na_{5/6}Li_{5/18}Mn_{13/18}O_2$ materials, and software programming to process and present collected data. F.D. synthesized the Na-Li-Cu-Fe-Mn-O materials. Z.Y., B.S.-L., and A.A.-G. predict Na-ion layered oxides tested by cationic potential. J.W. and X.B. performed STEM observation and analysis. C.Z., Q.W., Z.Y., M.W., Y.L., C.D., and Y.-S.H. wrote the manuscript. All authors participated in analyzing the experimental results and preparing the manuscript. C.Z., Q.W., and Z.Y. contributed equally to this work. **Competing interests:** All authors declare that they have no competing interests. **Data and materials availability:** All data are available in the main text or the supplementary materials.

SUPPLEMENTARY MATERIALS

science.sciencemag.org/content/370/6517/708/suppl/DC1
Materials and Methods
Supplementary Text
Figs. S1 to S15
Tables S1 to S19
References (*24*–*169*)

4 August 2019; accepted 18 September 2020
10.1126/science.aay9972

Rational design of layered oxide materials for sodium-ion batteries

Chenglong Zhao, Qidi Wang, Zhenpeng Yao, Jianlin Wang, Benjamín Sánchez-Lengeling, Feixiang Ding, Xingguo Qi, Yaxiang Lu, Xuedong Bai, Baohua Li, Hong Li, Alán Aspuru-Guzik, Xuejie Huang, Claude Delmas, Marnix Wagemaker, Liquan Chen and Yong-Sheng Hu

Science **370** (6517), 708-711.
DOI: 10.1126/science.aay9972

Layering the charge

Layered metal oxides such as lithium cobalt oxide have attracted great attention for rechargeable batteries. In lithium cells, only the octahedral structure forms, but in sodium cells, trigonal prismatic structures are also possible. However, there is a lack of understanding about how to predict and control the formation of each structure. Zhao *et al.* used the simple properties of ions, namely their charge and their radius appropriately weighted by stoichiometry, to determine whether sodium in the interlayers between the transition metal or other ion-oxide layers remain octahedral rather than switching over to trigonal prismatic coordination.

Science, this issue p. 708